Cumhuriyet Sci. J., 44(3) (2023) 547-560
DOI: https://doi.org/10.17776/csj.1293551

Cumhuriyet Science Journal

| csj.cumhuriyet.edu.tr | Founded: 2002 ISSN: 2587-2680 e-ISSN: 2587-246X Publisher: Sivas Cumhuriyet University

3D Stabilized FEM Solution of the MHD Equations in an External Medium and Around a Solid

Selçuk Han Aydın[1,a,*], Mahir Ceylan Erdoğan[1,b]

[1] *Department of Mathematics, Faculty of Science, Karadeniz Technical University, Trabzon, Türkiye*
**Corresponding author*

Research Article

History
Received: 06/05/2023
Accepted: 30/08/2023

ABSTRACT

In this study, we consider 3-D MagnetoHydroDynamic (MHD) flow problems with different configurations which are mathematically expressed by system of coupled partial differential equation with coupled boundary conditions. These equations are solved numerically using one of the most popular schemes named as the finite element method (FEM) with SUPG type stabilized version in order to obtain accurate and stable solutions especially for the high values of the problem parameters. Obtained numerical solutions are visualized in terms of figures by taking the 2-D slices of the 3-D data in order to emphasize the accuracy of the proposed formulation.

Keywords: 3D-FEM, Stabilization, MHD flow, Exterior medium, Conducting solid.

[a] *shaydin@ktu.edu.tr* *https://orcid.org/0000-0002-1419-9458* [b] *erdoganmahir@gmail.com* *https://orcid.org/0000-0001-9775-5271*

Introduction

Besides the recent developments in the numerical methods, the finite element method (FEM) is one of the oldest but still popular numerical scheme for the solution of the engineering and mathematical boundary value problems even defined in complex geometries. Therefore, many researchers are paid attention to generate the different version of FEM with the combination of other modern numerical schemes. As results of these attentions, thousands of papers and hundreds of books are produced in the academic literature. H-version, p-version, hp-adaptive version, scaled boundary finite element version, stabilized versions, discontinuous version, extended version and smoothed versions are the most known ones. In order to formulate the real life problems, 3D-FEM is well suited numerical scheme for the solutions of the problems that don't have the analytical result. Therefore addition to 2-D case, we will pay attention to 3-D FEM applications (see [1-16] and references therein).

Noticed that, after 20^{th} century many authors performed both analytical and numerical studies about MagnetoHydroDynamic (MHD) due to the it's applications in many different areas such as MHD ion propulsion, liquid-metal and cooling of nuclear reactors, power generation, etc. Derivation of the corresponding differential equations using the Navier-Stokes equations, Maxwell equations with the Lorentz force and the theory of the MHD can be found in [17-19].

It is known that the value of the Hartmann number that exist in the MHD flow equations is large for the case of strong magnetic applications in which case the corresponding equation becomes convection dominated. However, standard numerical methods have some numerical troubles in the sense of stability for these type of problems. The FEM has advantage that one can consider different stabilization techniques additional to the standard formulation. Streamline Upwind Petrov-Galerkin (SUPG) method [20] is one of the mostly preferred stabilization technique in which stable solutions are obtained by adding mesh-dependent terms to the standard Galerkin FEM formulation. Even there are many papers in different areas as applications of MHD and stabilized FEM, let's refer only a few of them on recent years [21-34] and references therein.

We first considered the solution of the 2-D version of the coupled MHD equation which is firstly introduced in [35] with magnetic induction of exterior region using the Boundary Element Method (BEM) in [36] and DRBEM [37]. Then FEM-BEM coupling approach with stabilization is applied to the extended version of the problem by considering an insulated solid inside the fluid case in [38]. As a further stage, we decided to consider the 3-D version of the same problem. Firstly, as a 3-D application of FEM-BEM coupling approach is applied by Han Aydın in [39]. After giving the details of the stabilization in 3-D FEM in [40], this study is prepared as the next step application of the most general case of the coupled MHD problem in 3-D domains. Another contribution of this study to the literature beside the 3-D stabilized FEM application is obtaining the accurate solutions of the huge sized sparse systems using open source libraries. Therefore, as our knowledge, this study will fill the gap

on literature in this research area and demonstrate FEM only solution of the MHD equations.

The rest of the paper is organized as follows: The following section describes the mathematical modeling and FEM formulation of the considered 3 different cases with the addition stabilized terms0. In Numerical Results and Discussion we will display the figures of the obtained numerical solutions with required explanations. Finally, some concluding remarks are provided in the last section.

Mathematical Modeling

Mathematical modeling of the considered MHD flow problem can be derived using Navier-Stokes equations and Maxwell equations from electromagnetic theory using also the Ohm's law. Before writing the corresponding coupled system of partial differential equations, let's define some notations. The subscripts s, f [or F] and e corresponds to solid, fluid and external medium, respectively. Then the solid domain is $\Omega_s \in IR^3$, the fluid domain is $\Omega_f \in IR^3$ and the domain of the external medium is $\Omega_e \in IR^3$. Similarly, the normal vectors are also defined as n_s, n_f, n_e. The parameters Re, Rh, Rm_s, Rm_f and Rm_e are the Reynolds number, magnetic pressure, magnetic Reynolds number of the solid, magnetic Reynolds number of the fluid and magnetic Reynolds number of the external medium, respectively.

We consider 3 different problem configurations in the context of this study as;

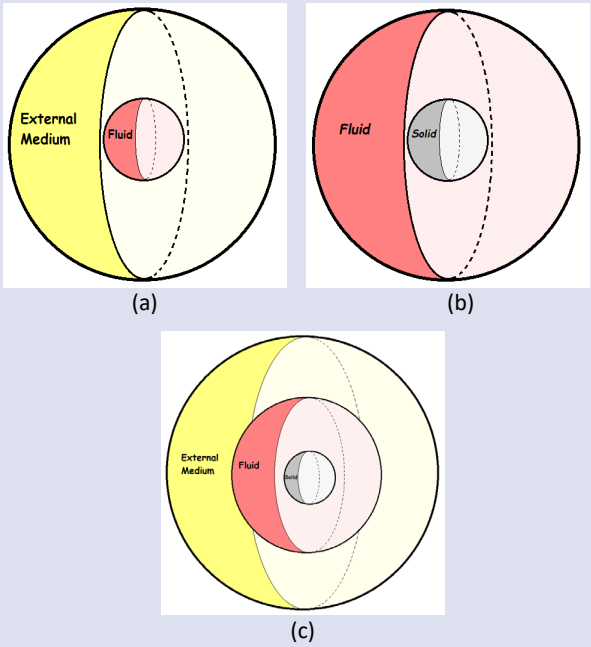

Figure 1. Problem configurations for different three cases

Case 1: Fluid inside an external medium

This is the first case of the considered MHD problem. We assume that the fluid is through the domain $\Omega_f$due to the constant pressure gradiend and the fluid is viscous, incompressible and electrically conducting. Also there is an externally applied magnetic field with an intensity $B_0$where it's direction through x axis with and angle β and through z axis with and angle α. The fluid domain is surrounded with an electrically conducting external domain Ω_e Figure 1(a). Then the system of coupled partial differential equations are defined as [39].

$$\left.\begin{aligned} \nabla^2 V^f + Re \cdot Rh \cdot (sin\,\alpha\, cos\,\beta \frac{\partial B^f}{\partial x} + sin\,\alpha\, sin\,\beta \frac{\partial B^f}{\partial y} + cos\,\alpha \frac{\partial B^f}{\partial z}) = -1 \\ \nabla^2 B^f + Rm_f \cdot (sin\,\alpha\, cos\,\beta \frac{\partial V^f}{\partial x} + sin\,\alpha\, sin\,\beta \frac{\partial V^f}{\partial y} + cos\,\alpha \frac{\partial V^f}{\partial z}) = 0 \end{aligned}\right\} \quad in\ \Omega_f \tag{1}$$

$$\nabla^2 B^e = 0 \quad in\ \Omega_e \tag{2}$$

with the boundary conditions

$$\left.\begin{aligned} V^f = 0 \\ B^e = B^f \\ \frac{1}{Rm_e}\frac{\partial B^e}{\partial n_e} = \frac{1}{Rm_f}\frac{\partial B^f}{\partial n_f} \end{aligned}\right\} \quad \in \partial\Omega_f \cap \partial\Omega_e = \Gamma_{fe}\,. \tag{3}$$

Noticed that even the external medium is unbounded, due to the FEM formulation, we need to define an artificial boundary on the outer side of the external domain Ω_e as $\Gamma_e$for the domain discretization where either $B^e = 0$ (known as the Drichlet type boundary condition) or $\frac{\partial B^e}{\partial n_e} = 0$ (Neumann type boundary condition) are specified on that boundary. The Drichlet type boundary condition is compatible with the behavior of the real potential solution of B^e such that it is assumed that $B^e \to 0$ as $[x^2 + y^2 + z^2] \to \infty$which is called as Saint-Venant principle [36]. Similarly, the Neumann type boundary condition corresponds to the free exit behavior of the induced magnetic field. However, if this type of boundary condition is specified, induced magnetic field solutions can be obtained up to a constant. Therefore, in order to obtain a unique solution, the obtained induced magnetic values should be normalized by using the identity

$$\iiint_\Omega B d\Omega = 0 \tag{4}$$

where $B = B^s \cup B^f \cup B^e$.

Case 2: Fluid around a solid

As a second case, we assume that there is an electrically conducting solid inside the fluid having the domain Ω_s (Figure 1(b)). The rest of the fluid conditions are all same as in the previous case. Then, the system of equations and the boundary conditions are written as;

$$\nabla^2 B^s = 0 \quad in\ \Omega_s \tag{5}$$

$$\left.\begin{aligned} \nabla^2 V^f + Re \cdot Rh \cdot (\sin\alpha\cos\beta\frac{\partial B^f}{\partial x} + \sin\alpha\sin\beta\frac{\partial B^f}{\partial y} + \cos\alpha\frac{\partial B^f}{\partial z}) = -1 \\ \nabla^2 B^f + Rm_f \cdot (\sin\alpha\cos\beta\frac{\partial V^f}{\partial x} + \sin\alpha\sin\beta\frac{\partial V^f}{\partial y} + \cos\alpha\frac{\partial V^f}{\partial z}) = 0 \end{aligned}\right\} \quad in\ \Omega_f \tag{6}$$

with the coupled boundary conditions on the intersection of the fluid and solid domains as

$$\left.\begin{aligned} V^f = 0 \\ B^f = B^s \\ \frac{1}{Rm_f}\frac{\partial B^f}{\partial n_f} = \frac{1}{Rm_s}\frac{\partial B^s}{\partial n_s} \end{aligned}\right\} \quad \in \partial\Omega_f \cap \partial\Omega_s = \Gamma_{sf} \tag{7}$$

and additionally we assume that the exterior side of the fluid domain is insulated so $B^f = 0$ on that boundary.

Case 3: Fluid around a solid and inside an external medium

Finally, in the third case which is the combination of the first two cases, we consider a fluid both inside an electrically conducting exterior medium and around a conducting medium Figure 1(c). Then the full system of equations are written as:

$$\nabla^2 B^s = 0 \quad in\ \Omega_s \tag{8}$$

$$\left.\begin{aligned} \nabla^2 V^f + Re \cdot Rh \cdot (\sin\alpha\cos\beta\frac{\partial B^f}{\partial x} + \sin\alpha\sin\beta\frac{\partial B^f}{\partial y} + \cos\alpha\frac{\partial B^f}{\partial z}) = -1 \\ \nabla^2 B^f + Rm_f \cdot (\sin\alpha\cos\beta\frac{\partial V^f}{\partial x} + \sin\alpha\sin\beta\frac{\partial V^f}{\partial y} + \cos\alpha\frac{\partial V^f}{\partial z}) = 0 \end{aligned}\right\} \quad in\ \Omega_f \tag{9}$$

$$\nabla^2 B^e = 0 \quad in\ \Omega_e \tag{10}$$

with the boundary conditions on the intersection of the fluid and solid domains as

$$\left.\begin{aligned} V^f = 0 \\ B^f = B^s \\ \frac{1}{Rm_f}\frac{\partial B^f}{\partial n_f} = \frac{1}{Rm_s}\frac{\partial B^s}{\partial n_s} \end{aligned}\right\} \quad \in \partial\Omega_f \cap \partial\Omega_s = \Gamma_{sf} \text{ and } \left.\begin{aligned} V^f = 0 \\ B^e = B^f \\ \frac{1}{Rm_e}\frac{\partial B^e}{\partial n_e} = \frac{1}{Rm_f}\frac{\partial B^f}{\partial n_f} \end{aligned}\right\} \quad \in \partial\Omega_f \cap \partial\Omega_e = \Gamma_{fe} \tag{11}$$

and similar to the first case, on Γ_e either $B^e = 0$or $\frac{\partial B^e}{\partial n_e} = 0$.

FEM Formulation

As a first step we will reformulate the given equation in the fluid domain by change of a new variable B^Fas $B^F = \frac{Re\cdot Rh\cdot B^f}{Ha}$ where $Ha = \sqrt{Re \cdot Rh \cdot Rm_f}$ is the Hartmann number of the fluid. Then the equations are written in the new form as [39]

$$\left.\begin{aligned} \nabla^2 V^f + \left[M_x\frac{\partial B^F}{\partial x} + M_y\frac{\partial B^F}{\partial y} + M_z\frac{\partial B^F}{\partial z}\right] = -1 \\ \nabla^2 B^F + \left[M_x\frac{\partial V^f}{\partial x} + M_y\frac{\partial V^f}{\partial y} + M_z\frac{\partial V^f}{\partial z}\right] = 0 \end{aligned}\right\} \ in\ \Omega_f \tag{12}$$

for $M_x = Ha\sin\alpha\cos\beta$, $M_y = Ha\sin\alpha\sin\beta$ and $M_z = Ha\cos\alpha$. Then as a second step, we will decouple these coupled equations using the following transformation by defining the new variables $U_1(x,y,z)$ and $U_2(x,y,z)$ as

$$\begin{aligned} U^1 &= V^f + B^F, \\ U^2 &= V^f - B^F, \end{aligned} \tag{13}$$

then equations become

$$\nabla^2 B^s = 0 \quad in\ \Omega_s \tag{14}$$

$$\left.\begin{aligned} \nabla^2 U^1 + M\cdot\nabla U^1 &= -1 \\ \nabla^2 U^2 - M\cdot\nabla U^2 &= -1 \end{aligned}\right\} in\ \Omega_f \tag{15}$$

$$\nabla^2 B^e = 0 \quad in\ \Omega_e \tag{16}$$

where $M = (M_x, M_y, M_z)$.

Before obtaining the finite element formulation of the given equations, let's define the required function spaces.

- $L^2(\Omega)$: the space of square integrable functions over the domain Ω,
- $H^1(\Omega)$: the Sobolev space of $L^2(\Omega)$ functions whose derivatives are square integrable functions in Ω,
- $H_0^1(\Omega)$: the Sobolev subspace of $H^1(\Omega)$ functions in Ω with zero value on the boundary $\partial\Omega$.

In order to construct the FEM formulation, the problem domain should be partitioned to the elements (linear tetrahedron elements in our computations) in a standard way (e.g. no overlapping, no vertex on the edge or side of a neighboring elements, etc). Then, we can obtain the standard Galerkin FEM weak formulation to the these decoupled system of equations by employing the linear function space $L = (H_0^1(\Omega))^2$ as: Find $\{B^s; U^1; U^2; B^e\} \in \{L\times L\times L\times L\}$ such that

$$\begin{aligned} &a(\nabla B^s, \nabla s) - \ell(\frac{\partial B^s}{\partial n_s}, s) + a(\nabla U^1, \nabla w^1) - b(M_x\frac{\partial U^1}{\partial x} + M_y\frac{\partial U^1}{\partial y} + M_z\frac{\partial U^1}{\partial z}, w^1) - \ell(\frac{\partial U^1}{\partial n_f}, w^1) \\ &\quad + a(\nabla U^2, \nabla w^2) + b(M_x\frac{\partial U^2}{\partial x} + M_y\frac{\partial U^2}{\partial y} + M_z\frac{\partial U^2}{\partial z}, w^2) - \ell(\frac{\partial U^2}{\partial n_f}, w^2) + a(\nabla B^e, \nabla e) \\ &\quad - \ell(\frac{\partial B^e}{\partial n_e}, e) = b(1, w^1) + b(1, w^2) \end{aligned} \tag{17}$$

$\forall\{s; w^1; w^2; e\} \in \{L\times L\times L\times L\}$ where $a(\nabla u, \nabla v)$, $b(u,v)$ and $\ell(u,v)$ are the usual bi-linear and linear forms for the domain and boundary integrals such that

$$a(\nabla u, \nabla v) = \iiint_\Omega \left(\frac{\partial u}{\partial x}\frac{\partial v}{\partial x} + \frac{\partial u}{\partial y}\frac{\partial v}{\partial y} + \frac{\partial u}{\partial z}\frac{\partial v}{\partial z}\right) d\Omega, \quad b(u,v) = \iiint_\Omega (uv)\, d\Omega$$

and $\ell(\frac{\partial u}{\partial n}, v) = \iint_\Gamma \left(\frac{\partial u}{\partial n} v\right) d\partial\Omega$

Then, the variational formulation is written by the choice of finite dimensional subspaces $L_h \subset L$, defined by discretization of the domain to the linear tetrahedron elements as [7]: Find $\{{B_h}^s; {U_h}^1; {U_h}^2; {B_h}^e\} \in \{L_h\times L_h\times L_h\times L_h\}$ such that

$$\begin{aligned} &a(\nabla {B_h}^s, \nabla s_h) - \ell(\frac{\partial {B_h}^s}{\partial n_s}, s_h) + a(\nabla {U_h}^1, \nabla {w_h}^1) - b(M_x\frac{\partial {U_h}^1}{\partial x} + M_y\frac{\partial {U_h}^1}{\partial y} + M_z\frac{\partial {U_h}^1}{\partial z}, {w_h}^1) - \ell(\frac{\partial {U_h}^1}{\partial n_f}, {w_h}^1) \\ &\quad + a(\nabla {U_h}^2, \nabla {w_h}^2) + b(M_x\frac{\partial {U_h}^2}{\partial x} + M_y\frac{\partial {U_h}^2}{\partial y} + M_z\frac{\partial {U_h}^2}{\partial z}, {w_h}^2) - \ell(\frac{\partial {U_h}^2}{\partial n_f}, {w_h}^2) \\ &\quad + a(\nabla {B_h}^e, \nabla e_h) - \ell(\frac{\partial {B_h}^e}{\partial n_e}, e_h) = b(1, {w_h}^1) + b(1, {w_h}^2) \end{aligned} \tag{18}$$

$\forall\{s_h; {w_h}^1; {w_h}^2; e_h\} \in \{L_h\times L_h\times L_h\times L_h\}$

$$a(\nabla {B_h}^s, \nabla s_h) - \ell(\frac{\partial {B_h}^s}{\partial n_s}, s_h) + a(\nabla {U_h}^1, \nabla {w_h}^1) - b(M_x \frac{\partial {U_h}^1}{\partial x} + M_y \frac{\partial {U_h}^1}{\partial y} + M_z \frac{\partial {U_h}^1}{\partial z}, {w_h}^1) - \ell(\frac{\partial {U_h}^1}{\partial n_f}, {w_h}^1)$$
$$+ \tau_K \cdot b(-M_x \frac{\partial {U_h}^1}{\partial x} - M_y \frac{\partial {U_h}^1}{\partial y} - M_z \frac{\partial {U_h}^1}{\partial z} - 1, -M_x \frac{\partial {w_h}^1}{\partial x} - M_y \frac{\partial {w_h}^1}{\partial y} - M_z \frac{\partial {w_h}^1}{\partial z})$$
$$+ a(\nabla {U_h}^2, \nabla {w_h}^2) + b(M_x \frac{\partial {U_h}^2}{\partial x} + M_y \frac{\partial {U_h}^2}{\partial y} + M_z \frac{\partial {U_h}^2}{\partial z}, {w_h}^2) - \ell(\frac{\partial {U_h}^2}{\partial n_f}, {w_h}^2) + \tau_K \quad (19)$$
$$\cdot b(M_x \frac{\partial {U_h}^2}{\partial x} + M_y \frac{\partial {U_h}^2}{\partial y} + M_z \frac{\partial {U_h}^2}{\partial z} - 1, M_x \frac{\partial {w_h}^2}{\partial x} + M_y \frac{\partial {w_h}^2}{\partial y} + M_z \frac{\partial {w_h}^2}{\partial z}) + a(\nabla {B_h}^e, \nabla e_h)$$
$$- \ell(\frac{\partial {B_h}^e}{\partial n_e}, e_h) = b(1, {w_h}^1) + b(1, {w_h}^2)$$

with the stabilization parameter

$$\tau_K = \begin{cases} \dfrac{h_K}{2Ha} \text{ if } Pe_k \geq 1 \\ \dfrac{h_K^2}{12} \text{ if } Pe_k < 1 \end{cases} \quad (20)$$

where h_K h_K is the diameter of the element Kwhich is calculated as the longest side of the corresponding tetrahedron element, $Pe_K = h_K \frac{Ha}{6}$ is the Peclet number.

Now, one can turn back to original unknowns with inverse transformations

$$V^f = \frac{U^1 + U^2}{2} \text{ and } B^F = \frac{U^1 - U^2}{2} \quad \rightarrow \quad B^f = \frac{Ha}{Re \cdot Rh} B^F \quad (21)$$

and since the coefficients $\frac{Rm_f}{Rm_e} \geq 1$ and $\frac{Rm_f}{Rm_s} \geq 1$, use the relations in the coupled boundary conditions as

$$\frac{\partial B^f}{\partial n_f} = \frac{Rm_f}{Rm_s} \frac{\partial B^s}{\partial n_s} \quad \text{and} \quad \frac{\partial B^f}{\partial n_f} = \frac{Rm_f}{Rm_e} \frac{\partial B^e}{\partial n_e} \quad (22)$$

Then one gets the final variational form of the equations as

$$a(\nabla {B_h}^s, \nabla s_h) - \ell(\frac{\partial {B_h}^s}{\partial n_s}, s_h) + a(\nabla {U_h}^1, \nabla {w_h}^1) - b(M_x \frac{\partial {U_h}^1}{\partial x} + M_y \frac{\partial {U_h}^1}{\partial y} + M_z \frac{\partial {U_h}^1}{\partial z}, {w_h}^1) - \ell(\frac{\partial {U_h}^1}{\partial n_f}, {w_h}^1) + \tau_K \cdot$$
$$b(-M_x \frac{\partial {U_h}^1}{\partial x} - M_y \frac{\partial {U_h}^1}{\partial y} - M_z \frac{\partial {U_h}^1}{\partial z} - 1, -M_x \frac{\partial {w_h}^1}{\partial x} - M_y \frac{\partial {w_h}^1}{\partial y} - M_z \frac{\partial {w_h}^1}{\partial z}) + a(\nabla {U_h}^2, \nabla {w_h}^2) + b(M_x \frac{\partial {U_h}^2}{\partial x} + \quad (23)$$
$$M_y \frac{\partial {U_h}^2}{\partial y} + M_z \frac{\partial {U_h}^2}{\partial z}, {w_h}^2) - \ell(\frac{\partial {U_h}^2}{\partial n_f}, {w_h}^2) + \tau_K \cdot b(M_x \frac{\partial {U_h}^2}{\partial x} + M_y \frac{\partial {U_h}^2}{\partial y} + M_z \frac{\partial {U_h}^2}{\partial z} - 1, M_x \frac{\partial {w_h}^2}{\partial x} + M_y \frac{\partial {w_h}^2}{\partial y} +$$
$$M_z \frac{\partial {w_h}^2}{\partial z}) + a(\nabla {B_h}^e, \nabla e_h) - \ell(\frac{\partial {B_h}^e}{\partial n_e}, e_h) = b(1, {w_h}^1) + b(1, {w_h}^2)$$

We will obtain the system of linear equations in matrix-vector forms

Case 1:
$$\begin{bmatrix} K+S & -Re \cdot Rh \cdot C & 0 \\ -Rm_f \cdot C & K+S & -\frac{Rm_f}{Rm_e} \cdot Q \\ 0 & 0 & K \end{bmatrix} \begin{Bmatrix} V^f \\ B^f \\ B^e \end{Bmatrix} = \begin{Bmatrix} R_1 \\ R_2 \\ 0 \end{Bmatrix} \quad (24)$$

Case 2:
$$\begin{bmatrix} K & 0 & 0 \\ 0 & K+S & -Re \cdot Rh \cdot C \\ -\frac{Rm_f}{Rm_s} \cdot Q & -Rm_f \cdot C & K+S \end{bmatrix} \begin{Bmatrix} B^s \\ V^f \\ B^f \end{Bmatrix} = \begin{Bmatrix} 0 \\ R_1 \\ R_2 \end{Bmatrix} \quad (25)$$

Case 3:
$$\begin{bmatrix} K & 0 & 0 & 0 \\ 0 & K+S & -Re \cdot Rh \cdot C & 0 \\ -\frac{Rm_f}{Rm_s} \cdot Q & -Rm_f \cdot C & K+S & -\frac{Rm_f}{Rm_e} \cdot Q \\ 0 & 0 & 0 & K \end{bmatrix} \begin{Bmatrix} B^s \\ V^f \\ B^f \\ B^e \end{Bmatrix} = \begin{Bmatrix} 0 \\ R_1 \\ R_2 \\ 0 \end{Bmatrix} \quad (26)$$

where K, C, S and Q are the matrices and R_1 and R_2 are the vectors with the entries

$$K_{ij} = \iiint_\Omega \left(\frac{\partial N_i}{\partial x} \frac{\partial N_j}{\partial x} + \frac{\partial N_i}{\partial y} \frac{\partial N_j}{\partial y} + \frac{\partial N_i}{\partial z} \frac{\partial N_j}{\partial z} \right) d\Omega,$$

$$C_{ij} = \iiint_{\Omega} \left(M_x \frac{\partial N_i}{\partial x} + M_y \frac{\partial N_i}{\partial y} + M_z \frac{\partial N_i}{\partial z} \right) N_j d\Omega, \quad Q_{ij} = \iint_{\Gamma} \frac{\partial N_i}{\partial n} N_j d\,\partial\Omega,$$

$$S_{ij} = \iiint_{\Omega} \tau_K \left(M_x \frac{\partial N_i}{\partial x} + M_y \frac{\partial N_i}{\partial y} + M_z \frac{\partial N_i}{\partial z} \right) \left(M_x \frac{\partial N_j}{\partial x} + M_y \frac{\partial N_j}{\partial y} + M_z \frac{\partial N_j}{\partial z} \right) d\Omega,$$

$$R_{1_i} = \iiint_{\Omega} N_i d\Omega, \quad R_{2_i} = \iiint_{\Omega} \tau_K \left(M_x \frac{\partial N_i}{\partial x} + M_y \frac{\partial N_i}{\partial y} + M_z \frac{\partial N_i}{\partial z} \right) d\Omega.$$

One can obtain the all unknown values from the solution of these system of linear equations. Noticed that, due to the structure of the FEM formulation, obtained linear system of equations are in sparse form. Therefore it is better to solve the system using an efficient sparse solver.

Highlights of the Algorithm

- Initialize the parameters and the problem domain.
- Calculate the element matrices and vectors using the stabilized formulation (if the element is on the fluid domain) and apply the global matrix contribution.
- Apply the boundary conditions
- Solve the obtained system using Umfpack sparse solver.

Numerical Results and Discussion

In this section, we will demonstrate the proposed numerical scheme over some test problems in terms of the contour line figures as 2-D slices of the 3-D domain solutions. The problem domains are selected as $\Omega_s = \{(x,y,z) \,|\, x^2 + y^2 + z^2 \le 1\}$, $\Omega_f = \{(x,y,z) \,|\, x^2 + y^2 + z^2 \le 1\}$ for Case1 and $\Omega_f = \{(x,y,z) \,|\, 1 \le x^2 + y^2 + z^2 \le 4\}$ for Cases 2 and 3 and $\Omega_e = \{(x,y,z) \,|\, 1 \le x^2 + y^2 + z^2 \le 4\}$ for Case 1 and $\Omega_e = \{(x,y,z) \,|\, 4 \le x^2 + y^2 + z^2 \le 9\}$ for Case 3. For the comparision, we have also tested the cubic domain for Case1 as $\Omega_f = \{(x,y,z) \,|\, -1 \le x,y,z \le 1\}$ and $\Omega_e = \{(x,y,z) \,|\, -2 \le x,y,z \le 2\} \setminus \Omega_f$. Additionally, all we know that the resulting coefficient matrix in FEM formulation is in sparse form and its size is too large for the 3-D domain problems especially for the Case 3. On the numerical implementation side, user modified version of an open source sparse solver UMFPACK with long integer data types for the large sized systems is used with OpenMP support in GNU Fortran compiler in order to reduce the storage size and the computational time. Finally, the domain integrals over the tetrahedron elements and and the boundary integrals over the triangular elements are calculated numerilcally using 5 points and 4 points numerical quadrature methods, respectively such that numerical values are equal to the analytical values of the integrals.

Effect of the stabilization:

Before giving the results for the considered cases, we want to display the effect of the stabilization. It is seen from Figure 2 that even over the rough mesh and high values of the problem parameters ($\mathrm{Re} = 10,\ Rh = 10,\ Rm_f = 100$), there are some instabilities and oscillations on the solution contours obtained from standard Galerkin FEM formulation (left sub-figures (a) and (c)), the stabilized formulation eliminates these numerical difficulties (right sub-figures (b) and (d)) especially on the velocity solutions.

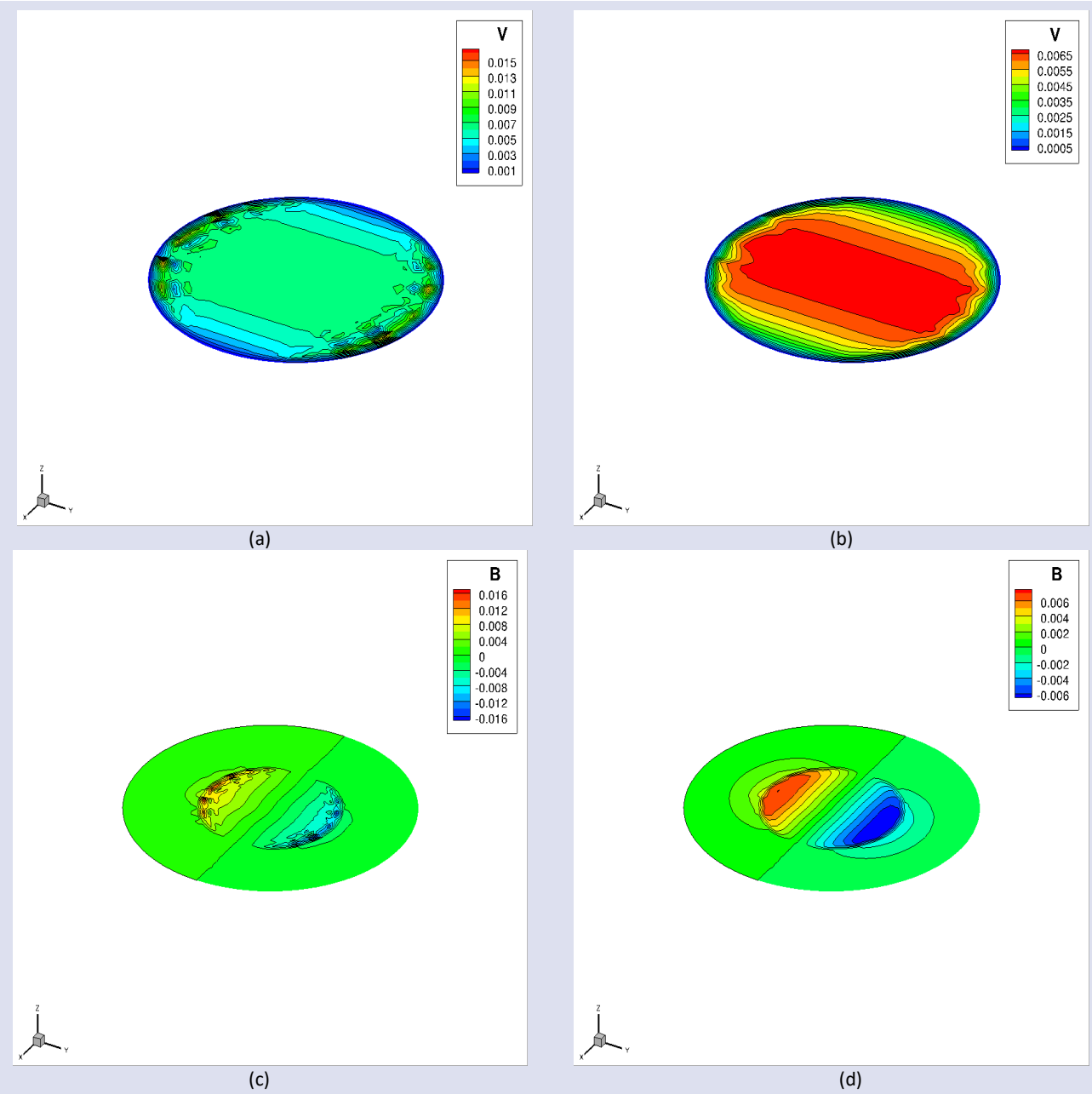

Figure 2. Velocity (a-b) and induced magnetic field (c-d) contour lines for different $x-y-z$ slices for $Re=10, Rh=10, Rm_f=100, Rm_e=1, \alpha=\pi/2, \beta=\pi/2$.

Case 1:

In this subsection, we displayed the effect of ratio of $\frac{Rm_f}{Rm_e}$ on the contour lines of the induced magnetic field solutions. It is seen from Figure 3 that even the continuity requirement is satified, there is a strong change on the intersection of the fluid and external domain boundary. Due to the Drichlet type boundary condition, contour lines close themselves on the exterior side of the external domain. Velocity contour lines are also compatible with the 2-D case of the considered MHD problem.

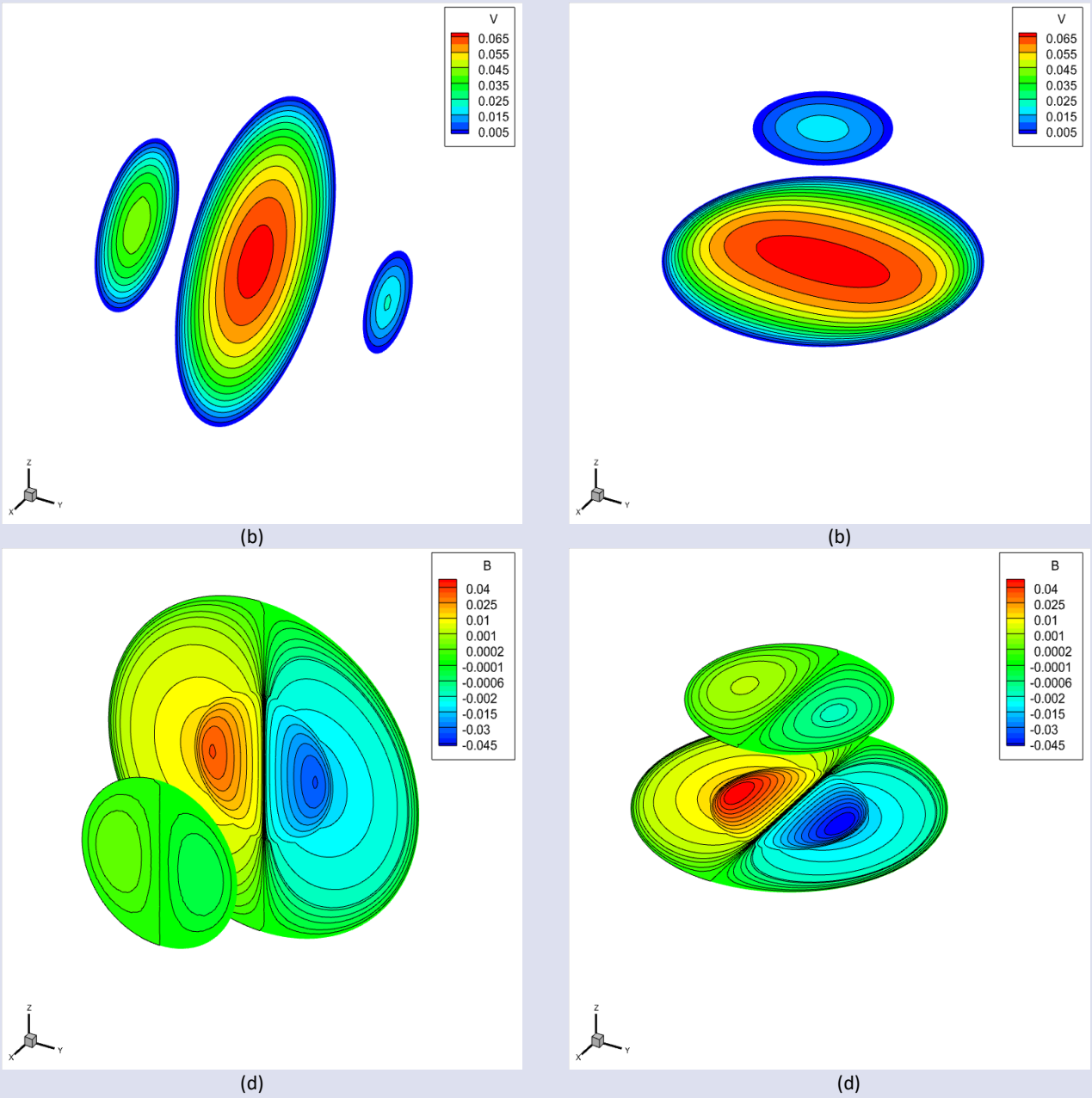

Figure 3. Velocity (a-b) and induced magnetic field (c-d) contour lines for different $x-y-z$ slices for $Re=10, Rh=1, Rm_f=10, Rm_e=1, \alpha=\pi/2, \beta=\pi/2$.

For the comparison, the same problem configuration is considered for the cubic domain in Figure 4 as defined above. Noticed that the behavior of the both spherical and cubic domains are similar to each other except the numerical difficulties at the corners on the induced magnetic field solution lying on the exterior region as predicted.

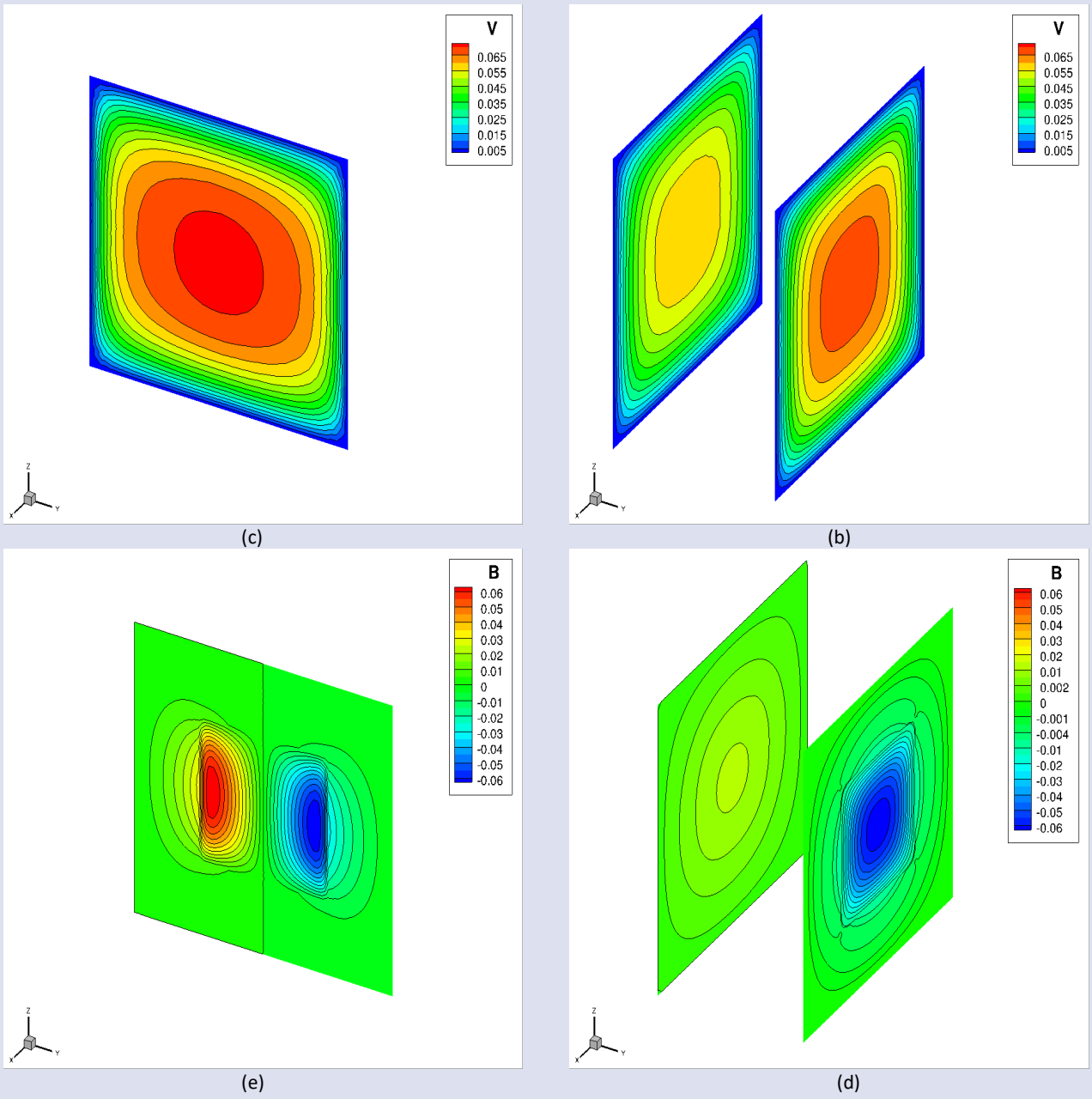

Figure 4. Velocity (a-b) and induced magnetic field (c-d) contour lines for different $x-y-z$ slices for $Re=10, Rh=1, Rm_f=10, Rm_e=1, \alpha=\pi/2, \beta=\pi/2$.

In Figure 5, we tested the effect of Neumann type boundary condition, effect of the high value of the Hartmann number and also the effect of direction of the applied external magnetic field ($\alpha=\pi/2$, $\beta=\pi/4$). It is seen that there is a boundary layer formation where it's position is changing depending on the selected slice due to the value of β and the flow becomes stagnant. One can see that the contour lines of the induced magnetic field are perpendicular to the exterior boundary due to the effect of the Neumann type boundary condition.

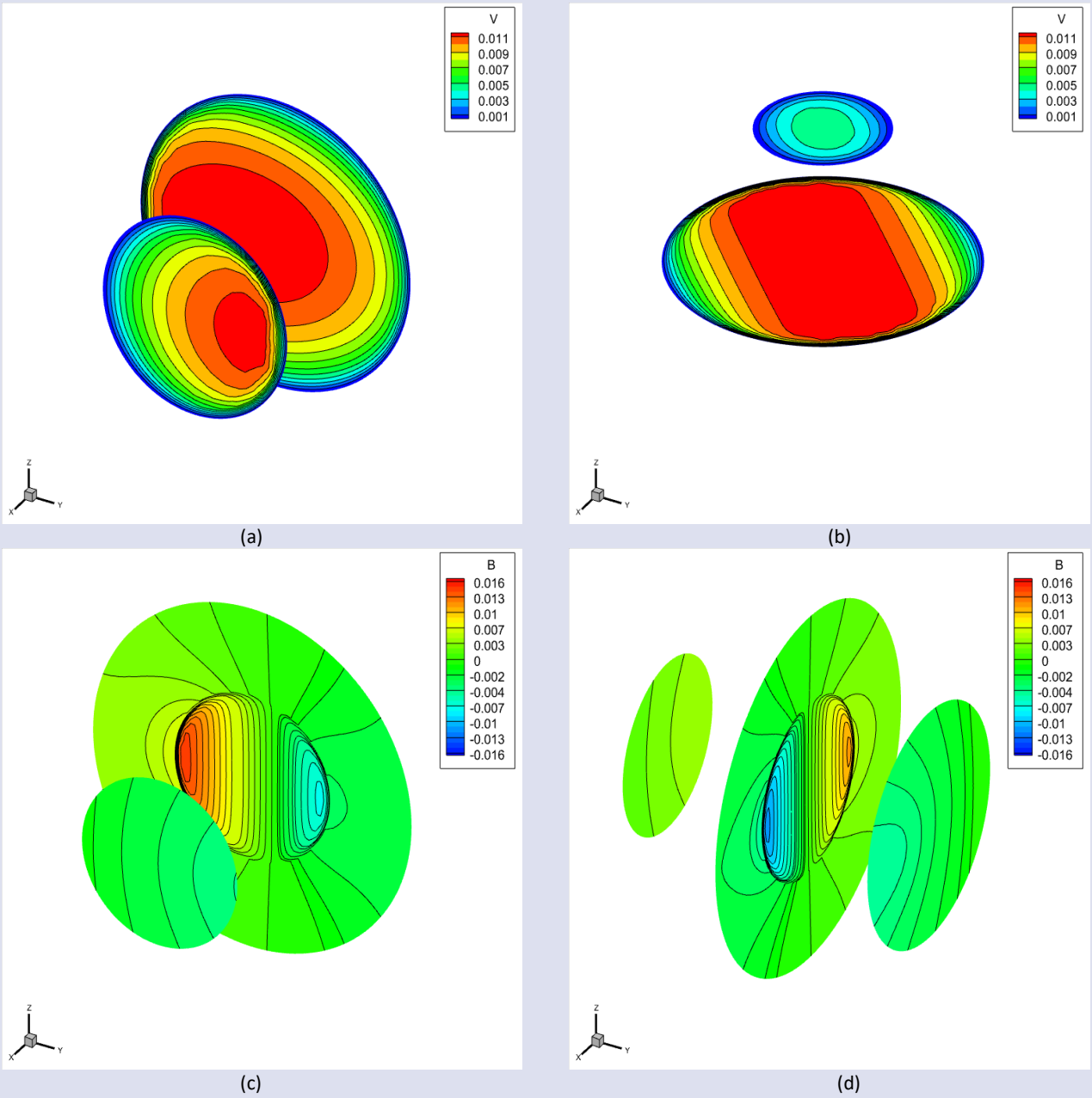

Figure 5. Velocity (a-b) and induced magnetic field (c-d) contour lines for different $x-y-z$ slices for $Re=10, Rh=5, Rm_f=50, Rm_e=1, \alpha=\pi/2, \beta=\pi/4$.

Case 2:

In order visualize the solid inside a fluid case, we selected the problem parameters as $Re=50, Rh=5, Rm_f=10, Rm_s=1, \alpha=\pi/2, \beta=0$. We want to display the effects of high values of problem parameters Re and Rh Rh on the flow behavior. It is seen that contour lines of both velocity and induced magnetic field are parallel with direction of the externally applied magnetic field due to the high value of the Hartmann number (see Figure 6).

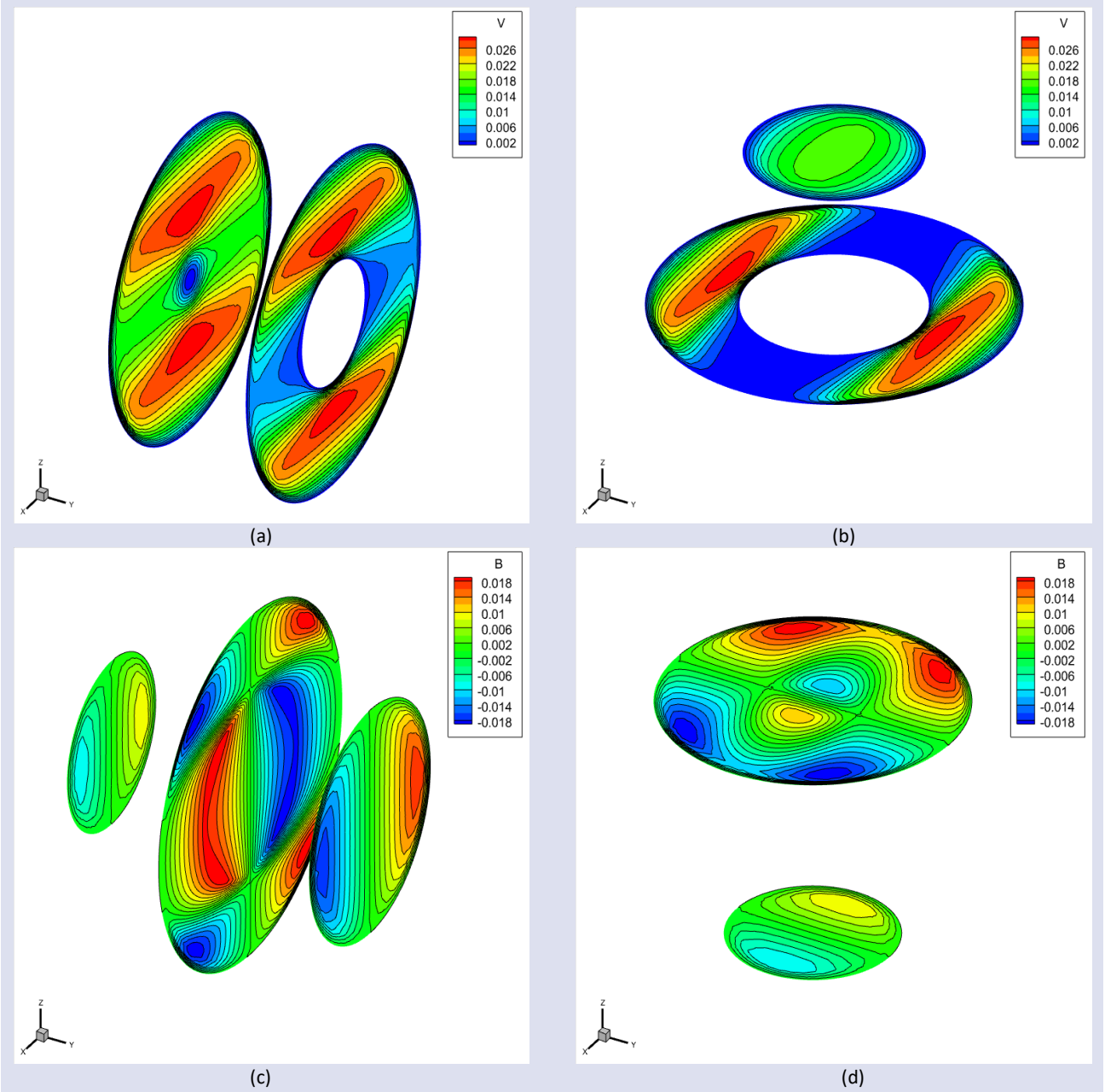

Figure 6. Velocity (a-b) and induced magnetic field (c-d) contour lines for different $y-z$ slices for $Re=50, Rh=5, Rm_f=10, Rm_s=1, \alpha=\pi/2, \beta=0$.

Case 3:

Finally, let's display the numerical solutions for the most general case. In Figure 7, we selected the problem parameters $Rm_s=1, Rm_f=1, Rm_e=1$ in order to display the smooth continuation of the contour lines of induced magnetic field solutions. It is also seen that the velocity takes it's maximum value at the center of the fluid domain as expected.

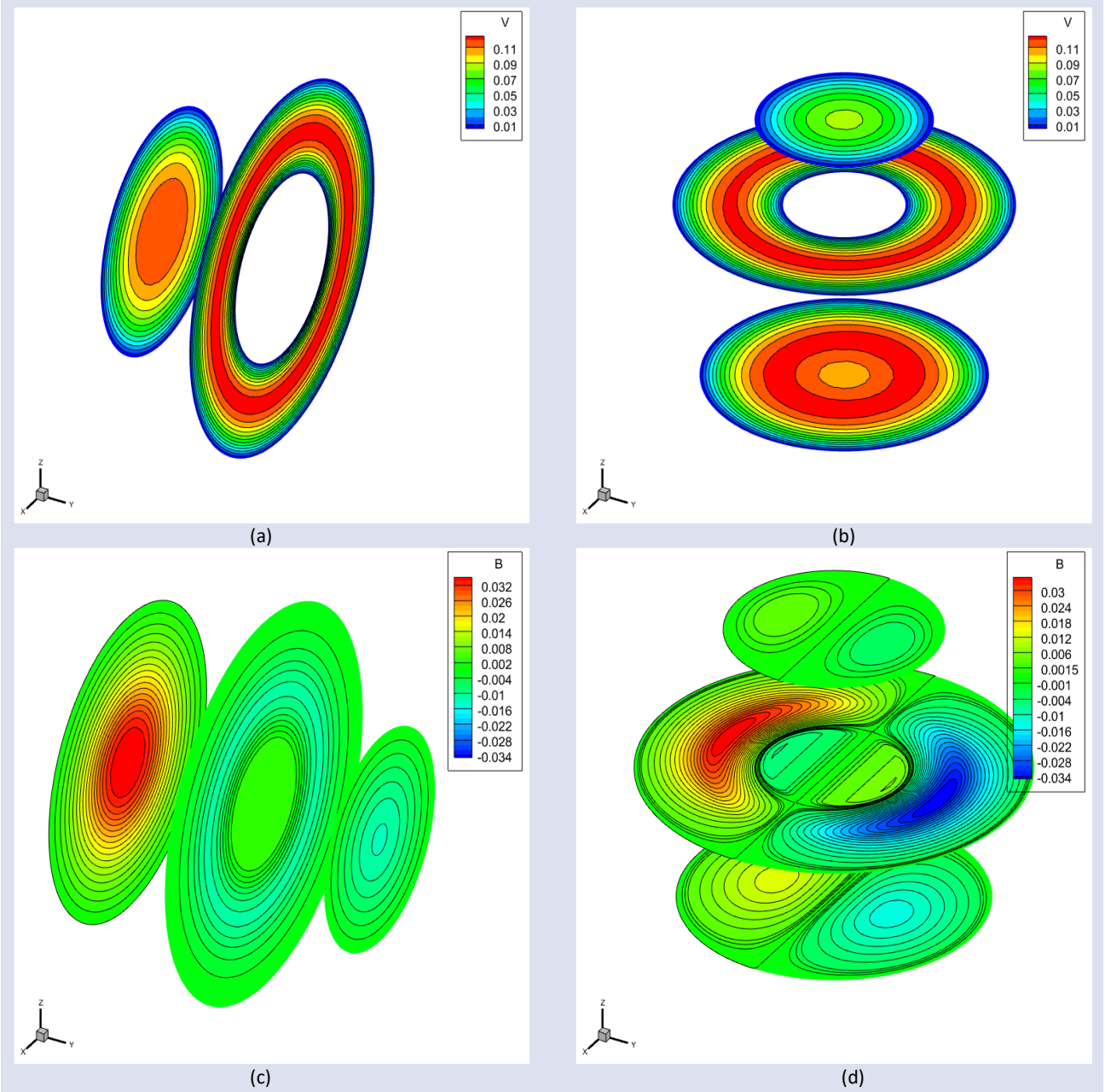

Figure 7. Velocity (a-b) and induced magnetic field (c-d) contour lines for different $y-z$ slices for $Re=1, Rh=1, Rm_s=1, Rm_f=1, Rm_e=1, \alpha=\pi/2, \beta=\pi/2$.

Additionally, in Figure 8, we have compared the induced magnetic field solutions for different problem parameters. One can see that contour lines are again parallel with the direction of B_0 and flow behavior is compatible with the literature results [36-39].

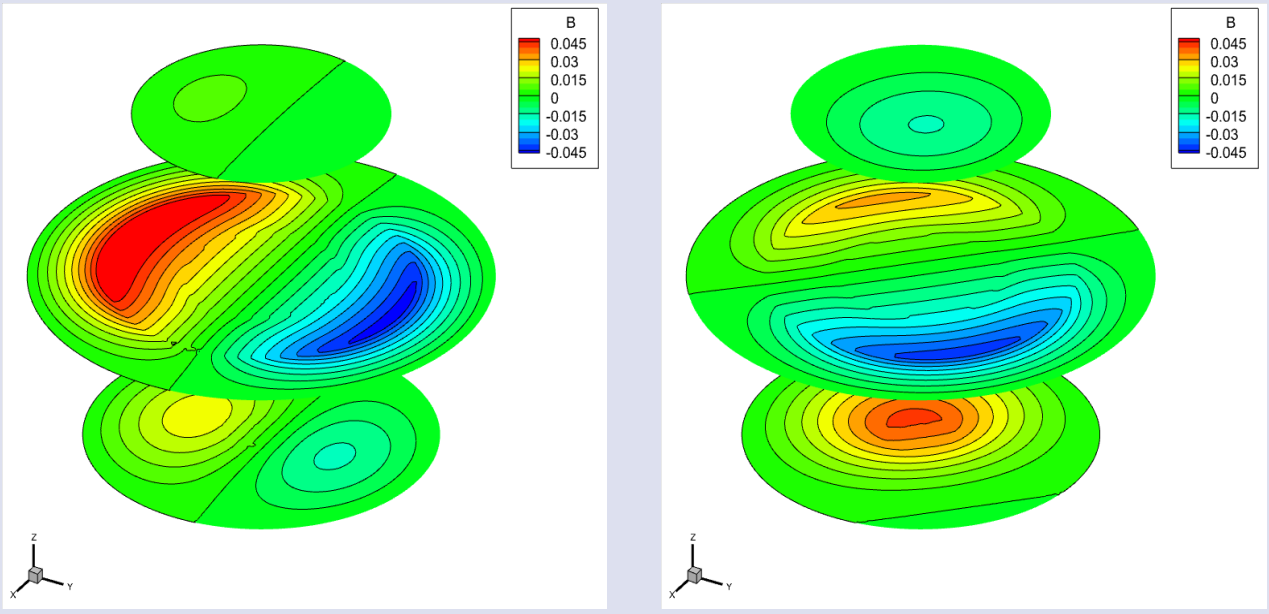

(a) (b)

Figure 8. Induced magnetic field contour lines for the y slice for $Re = 10, Rh = 1, Rm_s = 10, Rm_f = 100, Rm_e = 1, \alpha = \pi/2, \beta = \pi/2$ (a) and for $Re = 5, Rh = 5, Rm_s = 5, Rm_f = 50, Rm_e = 1, \alpha = \pi/4, \beta = \pi/4$ (b).

Conclusion

The SUPG typed stabilized FEM formulation of the 3-D MHD flow problem with three different problem configurations which have not been considered in the previous literature studies are provided in this study in a detail way. The proposed formulations are tested on some benchmark problems. Obtained solutions are displayed in terms of figures and one can see that the numerical solutions are stable and agree with the 2-D version of the similar problems.

Conflicts of interest

There are no conflicts of interest in this work.

Acknowledgments

The author wish to thank Prof. Dr. M. Tezer-Sezgin for her valuable support, comments and suggestions.

References

[1] Iwona A.W., Lucyna B., Lukasz D., Marek M., Stanislaw H.I., Modelling 3D dynamics of offshore lattice jib cranes by means of the rigid finite element method, *Journal of Ocean Engineering and Marine Energy,* 9 (2023) 495-513.

[2] Saimi A., Bensaid I., Fellah A., Effect of crack presence on the dynamic and buckling responses of bidirectional functionally graded beams based on quasi-3D beam model and differential quadrature finite element method, *Archive of Applied Mechanics,* 93 (2023) 3131–3151.

[3] Joshi K.K., Kar V.R., Elastoplastic Behaviour of Multidirectional Porous Functionally Graded Panels: A Nonlinear FEM Approach, *Iran J. Sci. Technol. Trans. Mech. Eng.,* (2023).

[4] Shao Z., Li X.S., Xiang P., A new computational scheme for structural static stochastic analysis based on Karhunen–Loève expansion and modified perturbation stochastic finite element method, *Computational Mechanics*, 71 (2023) 917-933.

[5] Gatica G.N., Nunez N., Ruiz-Baier R., Mixed-Primal Methods for Natural Convection Driven Phase Change with Navier–Stokes–Brinkman Equations, *Journal of Scientific Computing*, 95 (2023) 79.

[6] Vantyghem G., Ooms T., Corte W.D., FEM modelling techniques for simulation of 3D concrete printing, (2020).

[7] Liu W.K., Li S., Park H.S., Eighty Years of the Finite Element Method: Birth, Evolution, and Future, *Arch. Computat. Methods Eng.*, 29 (2022) 4431-4453.

[8] Xu H., Zou D., Kong X., Hu Z., Study on the effects of hydrodynamic pressure on the dynamic stresses in slabs of high CFRD based on the scaled boundary finite-element method, *Soil Dynamics and Earthquake Engineering*, 88 (2016) 223–236.

[9] Hell S., Becker W., The scaled boundary finite element method for the analysis of 3D crack interaction, *Journal of Computational Science*, 9(7) (2015) 76–81.

[10] Anjos, G.R., Borhani,N., Mangiavacchi, N., Thome J.R., A 3D moving mesh Finite Element Method for two-phase flows, *Journal of Computational Physics*, 270 (2014) 366–377.

[11] Schott B., Wall W.A., A new face-oriented stabilized XFEM approach for 2D and 3D incompressible Navier-Stokes equations, *Comput. Methods Appl. Mech. Engrg.*, 276 (2014) 233–265.

[12] Gravenkamp H., Man H., Song C., Prager J., The computation of dispersion relations for three-dimensional elastic waveguides using the Scaled Boundary Finite Element Method, *Journal of Sound and Vibration*, 332 (2013) 3756–3771.

[13] Stephan E.P., Maischak M., Leydecker F., An hp-adaptive finite element/boundary element coupling method for electromagnetic problems, *Comput. Mech.*, 39 (2007) 673–680.

[14] Geramy A., Sharafoddin F., Abfraction: 3D analysis by means of the finite element method, *Dental Research*, 34(7) (2003) 526–533.

[15] Rachowicz W., Demkowicz L., An hp-adaptive finite element method for electromagnetics: Part II. A 3D implementation, *Int. J. Numer. Meth. Engng.*, 53 (2002) 147–180.

[16] Chakraborty S., Bhattacharyya B., An efficient 3D stochastic finite element method, *International Journal of Solids and Structures*, 39 (2002) 2465–2475.

[17] Hartmann J., Theory of the laminar flow of an electrically conductive liquid in a homogeneous magnetic field, *K. Dan. Vidensk. Selsk. Mat. Fys. Medd.*, 15(6) (1937) 1-28.

[18] Shercliff J.A., Steady motion of conducting fluids in pipes under transverse magnetic fields, *Math. Proc. Cambridge*, 49 (1953) 136–144.

[19] Dragoş L., Magnetofluid Dynamics, *Abacus Pres*, 1975, 92-99.

[20] Brooks A.N., Hughes T.J.R., Streamline upwind/Petrov-Galerkin formulations for convection dominated flows with particular emphasis on the incompressible Navier-Stokes equations, *Comput. Methods Appl. Mech. Engrg.*, 32 (1982) 199-259.

[21] Rao S., A Numerical Study on Unsteady MHD Williamson Nanofluid Flow past a Permeable Moving Cylinder in the presence of Thermal Radiation and Chemical Reaction, *Biointerface Research in Applied Chemistry*, 13(5) (2023) 436.

[22] Zhao Y., Global well-posedness for the compressible non-resistive MHD equations in a 3D infinite slab, *Nonlinear Analysis*, 227 (2023) 113162.

[23] Patel A., Bhattacharyay R., 3D Thermo-fluid MHD simulation in a complex flow geometry, *Fusion Engineering and Design*, 191 (2023) 113558.

[24] Wang Z., Liu H., Global well-posedness for the 3-D generalized MHD equations, *Applied Mathematics Letters*, 140 (2023) 108585.

[25] Tezer-Sezgin M., Aydın S.H., Stabilized FEM solution of MHD duct flow with conducting cracks in the insulation, *Journal of Computational and Applied Mathematics*, 4230 (2023) 114936.

[26] Aggul M., Eroglu F.G., Kaya S., Artificial compression method for MHD system in Elsässer variables, *Applied Numerical Mathematics*, 185 (2023) 72-87.

[27] Chen Y., Peng Y., Shi X., A new blowup criterion for a generalized Hall-MHD system concerning the deformation tensor, *Applied Mathematics Letters*, 140 (2023) 108567.

[28] Fu L., An Efficient Low-Dissipation High-Order TENO Scheme for MHD Flows, *Journal of Scientific Computing*, 90(1) (2022) 1-24.

[29] Faizan, M., Ali, F., Loganathan, K. Zaib, A., Reddy, C.A., Abdelsalam, S.I., Entropy analysis of sutterby nanofluid flow over a riga sheet with gyrotactic microorganisms and Cattaneo-Christov double diffusion, *Mathematics*, 10(17) (2022) 3157.

[30] Luo Y., Fan X., Kim C.N., MHD flows in a U-channel under the influence of the spatially different channel-wall electric conductivity and of the magnetic field orientation, *Journal of Mechanical Science and Technology*, 35 (2021) 4477-4487.

[31] Wang H., Chen L., Zhang N.M., Ni M.J., Numerical simulations of MHD flows around a 180-degree sharp bend under a strong transverse magnetic field, *Nuclear Fusion*, 61(12) (2011) 126069.

[32] Aydin S.H., Nesliturk A.I., Tezer-Sezgin M., Two-level finite element method with a stabilizing subgrid for the incompressible MHD equations, *International Journal for Numerical Methods in Fluids*, 62(2) (2010) 188–210.

[33] Nesliturk A.I., Tezer-Sezgin M., Finite element method solution of electrically driven magnetohydrodynamic flow, *Journal of Computational and Applied Mathematics*, 192 (2006) 339–352.

[34] Codina R., Silva N.H., Stabilized finite element approximation of the stationary magneto-hydrodynamics equations, *Computational Mechanics*, 38 (2006) 344–355.

[35] Lungu E., Pohoata A., Finite element-boundary element approach of MHD pipe flow, *Proc. of Conf. on Fluid Mech. and Technical Appl.*, Bucharest, Romania, 2005, 79-88.

[36] Tezer-Sezgin M., Han Aydın S., BEM Solution of MHD Flow in a Pipe Coupled with Magnetic Induction of Exterior Region, *Computing* 95(1) (2013) 751–770.

[37] Han Aydın S., Tezer-Sezgin M., DRBEM Solution of MHD Pipe Flow in a Conducting Medium, *Journal of Computational and Applied Mathematics*, 259(B) (2014) 720–729.

[38] Han Aydın S., Selvitopi H., Stabilized FEM-BEM coupled solution of MHD pipe flow in an unbounded conducting medium, *Engineering Analysis with Boundary Elements*, 87(2) (2018) 122–132.

[39] Aydin, S.H., Stabilized solution of the 3-D MHD flow problem with FEM-BEM coupling approach, *Engineering Analysis with Boundary Elements*, 140 (2022) 519–530.

[40] Aydın S.H., Erdoğan M.C., Stabilization in 3-D FEM and solution of the MHD equations, *Mathematical Methods in the Applied Sciences,* (2023).